

## Theoretical evaluation of structural and transport properties of liquid magnesium-zinc alloy

This article has been downloaded from IOPscience. Please scroll down to see the full text article.

1989 J. Phys.: Condens. Matter 1 8621

(<http://iopscience.iop.org/0953-8984/1/44/032>)

View [the table of contents for this issue](#), or go to the [journal homepage](#) for more

Download details:

IP Address: 171.66.16.96

The article was downloaded on 10/05/2010 at 20:51

Please note that [terms and conditions apply](#).

## Theoretical evaluation of structural and transport properties of liquid magnesium–zinc alloy

R V Gopala Rao and U Bandyopadhyay

Department of Physical Chemistry, Jadavpur University, Calcutta 700 032, West Bengal, India

Received 10 February 1989, in final form 2 June 1989

**Abstract.** The Percus–Yevick equation, with a perturbing square-well attractive tail, serves as the main guideline in the evaluation of partial structures (Ashcroft and Langreth) of Mg–Zn alloy. The total structure factors obtained from these partials are found to be in satisfactory agreement with experimental results. The isothermal compressibilities are calculated from these partials in the long-wave limit. An estimate of the Bhatia–Thornton structure factors is made. The linear trajectory principle due to Helfand is utilised to calculate the diffusion coefficients. The most important aspect of the study is that the alloy properties are predicted solely from the potential parameters of the pure elements.

### 1. Introduction

The most important property that characterises a fluid state is its structure factor. Liquids and liquid alloys are, in principle, large systems comprising hard spheres with attractive forces providing a uniform background energy. Such a system is visualised through the PY approximation for binary mixtures of rigid spheres [1, 2]. A simple perturbation treatment of the PY equation for hard spheres with a square-well attractive tail forms the effective framework for the evaluation of structural and transport properties of Mg–Zn alloy.

### 2. Theory

For binary mixtures the direct correlation function (DCF) can be defined as

$$C_{ij}(r) = \begin{cases} C_{ij}^0(r) & \text{for } 0 < r \leq \sigma_{ij} \\ -\frac{\varphi_{ij}(r)}{k_B T} = \frac{\varepsilon_{ij}}{k_B T} & \text{for } \sigma_{ij} \leq r \leq A_{ij}\sigma_{ij} \\ 0 & \text{for } r > A_{ij}\sigma_{ij} \end{cases} \quad (1)$$

where  $C_{ij}^0(r)$  represents the hard-sphere solution of the PY equation given by Lebowitz [2] for binary mixtures and  $\sigma_{ij}$ ,  $\varepsilon_{ij}$  and  $A_{ij}$  are respectively the diameter, depth and breadth of the square well used. The values of the mixed parameters are determined from the

Lorentz–Berthelot mixing rule. They are given by

$$\begin{aligned}\sigma_{12} &= \frac{\sigma_{11} + \sigma_{22}}{2} \\ \varepsilon_{12} &= (\varepsilon_{11} \varepsilon_{12})^{1/2} \\ A_{12} &= \frac{A_{11}\sigma_{11} + A_{22}\sigma_{22}}{\sigma_{11} + \sigma_{22}}.\end{aligned}\quad (2)$$

The solution of the PY equation [2] for binary mixtures of rigid spheres represents  $C_{ij}(r)$  in the region  $0 < r \leq \sigma_{ij}$  and a square-well potential represents  $C_{ij}(r)$  in the region  $\sigma_{ij} \leq r \leq A_{ij}\sigma_{ij}$ . The Fourier transform of  $C_{ij}(r)$  in the overall range  $0 < r \leq A_{ij}\sigma_{ij}$  is given by Rao and co-workers [3, 4]. The  $C_{ij}(k)$  are linearly related to the partial structure factors,  $S_{ij}(k)$  [5], by

$$S_{11}(k) = \left(1 - \rho_{11}C_{11}(k) - \frac{\rho_{11}\rho_{22}C_{12}^2(k)}{1 - \rho_{22}C_{22}(k)}\right)^{-1} \quad (3)$$

$$S_{22}(k) = \left(1 - \rho_{22}C_{22}(k) - \frac{\rho_{11}\rho_{22}C_{12}^2(k)}{1 - \rho_{11}C_{11}(k)}\right)^{-1} \quad (4)$$

$$S_{12}(k) = (\rho_{11}\rho_{12})^{1/2}C_{12}(k)[(1 - \rho_{11}C_{11}(k))(1 - \rho_{22}C_{22}(k)) - \rho_{11}\rho_{22}C_{12}^2(k)]^{-1}. \quad (5)$$

Here the densities of the components are determined from those of the pure elements by assuming the ideal law of mixing. Thus the densities of the two species present in the alloy at various concentrations are obtained from the equations [6]

$$\rho_{11} = \frac{C_1\rho_1^0\rho_2^0}{C_1(\rho_2^0 - \rho_1^0) + \rho_1^0} \quad (6)$$

$$\rho_{22} = \frac{(1 - C_1)\rho_1^0\rho_2^0}{C_1(\rho_2^0 - \rho_1^0) + \rho_1^0} \quad (7)$$

where  $\rho_1^0$  and  $\rho_2^0$  are the densities of the pure elements under the same condition, obtained from [7].

The total structure factor in terms of the partials is given by [8]

$$S(k) = \sum_{i=1}^2 \sum_{j=1}^2 C_i^{1/2} C_j^{1/2} \frac{f_i(k)f_j(k)}{C_1 f_1^2(k) + C_2 f_2^2(k)} S_{ij}(k) \quad (8)$$

where  $f_1(k)$  and  $f_2(k)$  are the atomic scattering factors and  $C_1$  and  $C_2$  are the atomic fractions of component 1 and 2. Here 1 corresponds to Mg and 2 to Zn.

In the long-wave limit, i.e. as  $k \rightarrow 0$ ,  $C_{ij}(k)$  can be written as

$$\rho_{ii}C_{ii}(0) = -24\eta_{ii} \left( \frac{a_i}{3} + \frac{b_i\sigma_{ii}}{4} + \frac{d\sigma_{ii}^3}{6} \right) + \frac{8\eta_{ii}\varepsilon_{ii}(A_{ii}^3 - 1)}{k_B T} \quad (9)$$

$$\begin{aligned}C_{12}(0) &= \frac{4\pi\varepsilon_{12}\sigma_{12}^3(A_{12}^3 - 1)}{3k_B T} - \frac{4\pi a_1\sigma_{12}^3}{3} - 4\pi\sigma_{11}^3 \\ &\times \left\{ \frac{b(\sigma_{11} + 2\sigma_{22})}{12} + \frac{d\sigma_{11}(3\sigma_{11} + 5\sigma_{22})}{10} + \frac{d\sigma_{11}^2(2\sigma_{11} + 3\sigma_{22})}{30} \right\}.\end{aligned}\quad (10)$$

The isothermal compressibility  $\chi_T$  for binary mixture is related to  $\rho_{ii}C_{ii}(0)$  and  $C_{12}(0)$  through the Kirkwood–Buff equation [9]

$$\chi_T = [1 - C_1\rho_{11}C_{11}(0) - C_2\rho_{22}C_{22}(0) - 2\rho C_1C_2C_{12}(0)]^{-1}/\rho k_B T. \quad (11)$$

The Bhatia–Thornton structure factors [10] in terms of correlation functions of fluctuations in (a) particle density (regardless of type)  $S_{NN}(k)$ , (b) the composition, i.e. the local concentration (in mole fraction)  $S_{CC}(k)$  and (c) the cross correlation between number and composition  $S_{NC}(k)$  are evaluated from the following linear equations:

$$S_{NN}(k) = [C_1S_{11}(k) + C_2S_{22}(k) + 2C_1^{1/2}C_2^{1/2}S_{12}(k)] \quad (12)$$

$$S_{CC}(k) = C_1C_2[C_2S_{11}(k) + C_1S_{22}(k) - 2(C_1C_2)^{1/2}S_{12}(k)] \quad (13)$$

$$S_{NC}(k) = C_1C_2 \left( S_{11}(k) - S_{22}(k) + \frac{S_{12}(k)(C_2 - C_1)}{(C_1C_2)^{1/2}} \right). \quad (14)$$

We evaluate the partial radial distribution function from the partial structure factor from the relation

$$h_{ij}(r) = g_{ij}(r) - 1 = \frac{1}{2\pi^2 r \rho} \int_0^\infty [S_{ij}(k) - \delta_{ij}] k \sin(kr) dk. \quad (15)$$

Using the linear trajectory principle of Helfand [11] for binary mixtures we obtain the diffusion coefficient of the  $i$ th species [12] as

$$D_i = k_B T / \mathcal{E}_i \quad (16)$$

where  $\mathcal{E}_i$ , the friction constant of the  $i$ th species, is essentially the sum of

- (a) the friction coefficient due to repulsive core interaction,  $\mathcal{E}_i^H$
- (b) the friction coefficient due to soft interaction,  $\mathcal{E}_i^S$ , and
- (c) the friction coefficient due to cross effects of hard and soft forces in the potential,  $\mathcal{E}_i^{SH}$ , i.e.

$$\mathcal{E}_i = \mathcal{E}_i^H + \mathcal{E}_i^S + \mathcal{E}_i^{SH} \quad (17)$$

where

$$\mathcal{E}_i^H = \sum_{j=1}^2 \frac{2}{3} \sigma_{ij}^2 g_{ij} \rho_{jj} (2\pi\mu_{ij} k_B T)^{1/2} \quad (18)$$

$$\mathcal{E}_i^S = - \sum_{j=1}^2 \frac{\rho_{jj}}{3} \left( \frac{2\pi\mu_{ij}}{k_B T} \right)^{1/2} \frac{1}{(2\pi)^2} \int_0^\infty k^3 V_{ij}^S(k) G_{ij}(k) dk \quad (19)$$

$$\mathcal{E}_i^{SH} = - \sum_{j=1}^2 \frac{2\rho_{jj}}{3} g_{ij} \left( \frac{2\mu_{ij}}{\pi k_B T} \right)^{1/2} \int_0^\infty [k\sigma_{ij} \cos k\sigma_{ij} - \sin k\sigma_{ij}] V_{ij}^S(k) dk. \quad (20)$$

Here  $\rho_{jj}$  is the number density of the species  $j$ ,  $G_{ij}(k)$  and  $V_{ij}^S(k)$  are the Fourier transforms of the total correlation function  $[g_{ij}(r) - 1]$  and the soft part of the potential, respectively:

$$G_{ij}(k) = [S_{ij}(k) - \delta_{ij}] (\rho_{ii}\rho_{jj})^{1/2} \quad (21)$$

$$V_{ij}^S(k) = \frac{4\pi\epsilon_{ij}}{k^3} [A_{ij}k\sigma_{ij} \cos(A_{ij}k\sigma_{ij}) - \sin(A_{ij}k\sigma_{ij}) - k\sigma_{ij} \cos(k\sigma_{ij}) + \sin(k\sigma_{ij})]. \quad (22)$$

$\mu_{ij}$ , the reduced mass, is related to the atomic masses  $M_i$  and  $M_j$  by

$$\mu_{ij} = \frac{M_i M_j}{M_i + M_j}. \quad (23)$$

### 3. Results and discussion

The total structure factors characterising the system are evaluated at eight different concentrations of Mg at a temperature 40 °C higher than the corresponding liquidus temperature. The potential parameters,  $\sigma_{ij}$ ,  $\epsilon_{ij}$  and  $A_{ij}$  are determined by fitting the structures of the respective pure metals with the experimental values at the first peak position. All the input parameters used in the present calculation are given in table 1.

Table 1. Input parameters.

Temperature (K)	$\sigma_{11}$ (Å)	$\sigma_{22}$ (Å)	$\epsilon_{11}/k_B$ (K)	$\epsilon_{22}/k_B$ (K)	$A_{11}$	$A_{22}$	$\rho_1^0$ (Å <sup>3</sup> )	$\rho_2^0$ (Å <sup>3</sup> )
926.0	2.47	2.50	540.0	250.0	1.66	1.93	0.0393	0.0619

It is observed from figure 1 that the structure factors of both pure Mg and Zn are in good agreement with experimental results [13]. The agreement is particularly good for Mg but for Zn the skewness of the structure factor is not well reproduced.

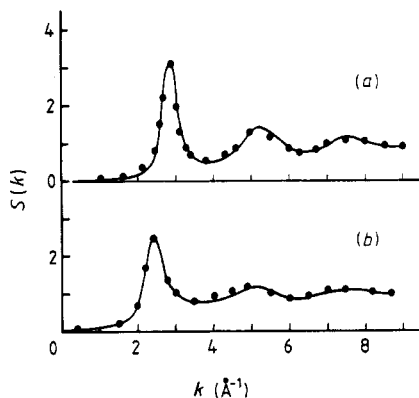
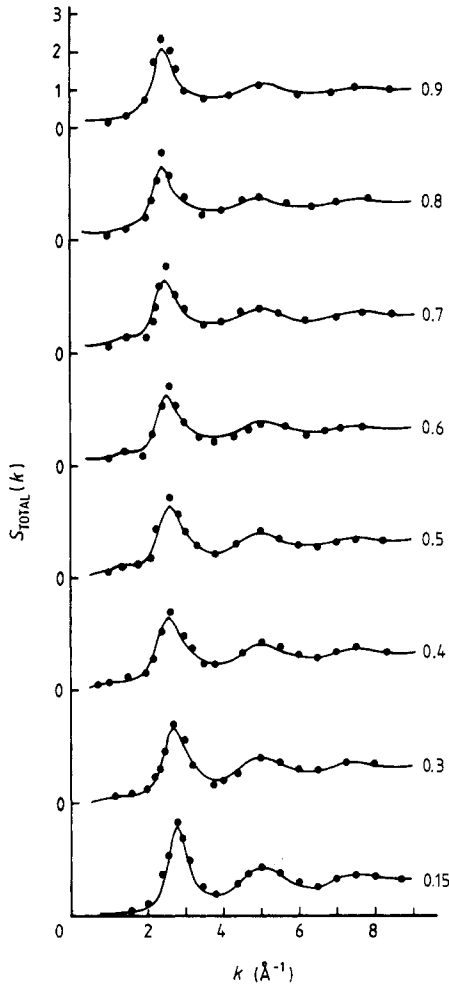
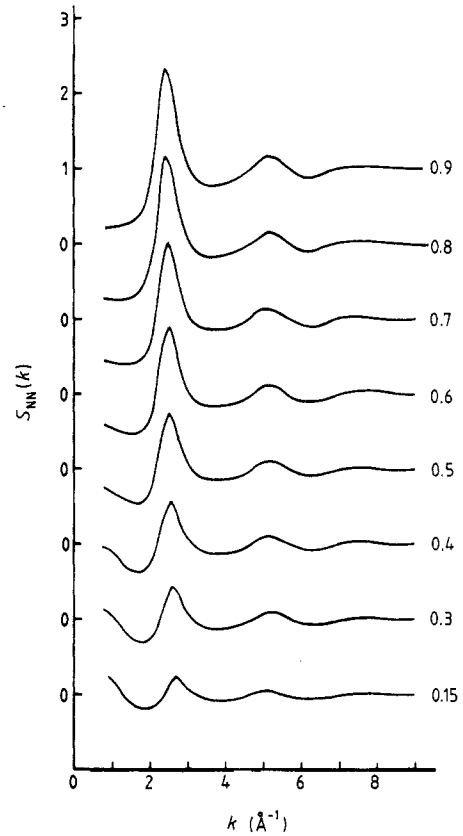


Figure 1. (a)  $S(k)$  against  $k$  for pure Zn; (b)  $S(k)$  against  $k$  for pure Mg; —, present calculated results; ···, experimental results.

In the present calculation, the concentrations are expressed in terms of atomic fractions of Mg, i.e.  $C_1$ . The total structure factors of the Mg–Zn melt are illustrated in figure 2 at eight different concentrations of Mg. We observe from figure 1 that the peak position of Mg has a lower  $k$  value compared with that of Zn. The total structure factor curves show a similar trend. Here, the maxima shift towards the larger  $k$  value with increase in Zn concentration in the melt. This has also been observed by Bühler *et al* [14]. The peak height decreases with increasing Mg concentration up to 60%. If the concentration of Mg increases still further, the peak height increases. This trend is also



**Figure 2.** Total structure factor  $S_{\text{TOTAL}}(k)$  against  $k$  for different atomic fractions of Mg for the Mg-Zn melt: —, present calculated results; ···, experimental results.



**Figure 3.**  $S_{\text{NN}}(k)$  against  $k$  for different atomic fractions of Mg for the Mg-Zn melt.

similar to that observed by Bühler *et al* [14]. Moreover there is a slight hint of a premaximum on the left-hand side of the main peak for  $30 < C_1 < 70\%$ . This peak in our calculation is not so pronounced as in the experimental one. But the hint definitely exists. The theoretical and experimental results are shown in table 2.

The Bhatia-Thornton structures,  $S_{\text{NN}}(k)$ ,  $S_{\text{CC}}(k)$  and  $S_{\text{NC}}(k)$  are plotted in figures 3, 4 and 5 for different atomic fractions of Mg. The variation of  $S_{\text{NN}}(k)$  with  $k$  is similar to that of the total structure factor. The peak height first decreases with increasing Mg concentration and then increases after 60%, as expected. Both  $S_{\text{CC}}(k)$  and  $S_{\text{NC}}(k)$  exhibit an oscillating nature. The former oscillates around the product of  $C_1$  and  $C_2$  and the latter around 0.

The direct correlation functions at the long-wave limit are utilised to calculate the isothermal compressibilities of Mg-Zn at different atomic fractions of Mg shown in

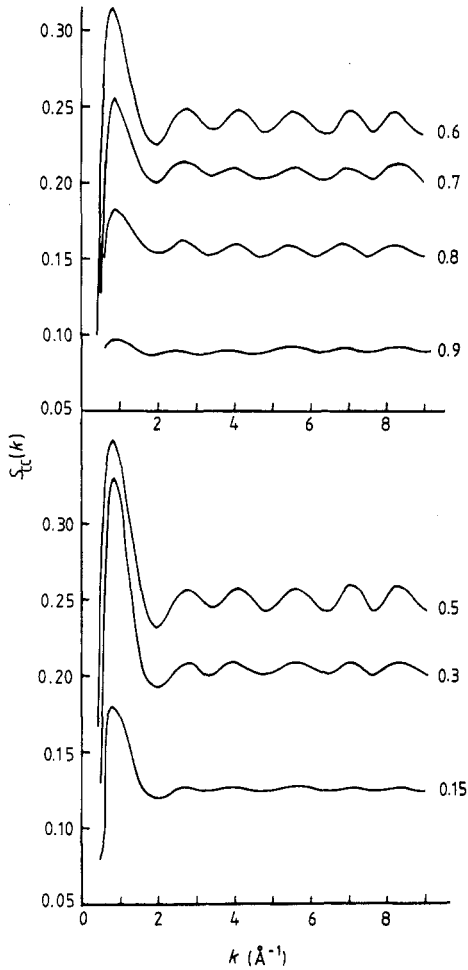


**Figure 4.**  $S_{CC}(k)$  against  $k$  for different atomic fractions of Mg for the Mg-Zn melt.

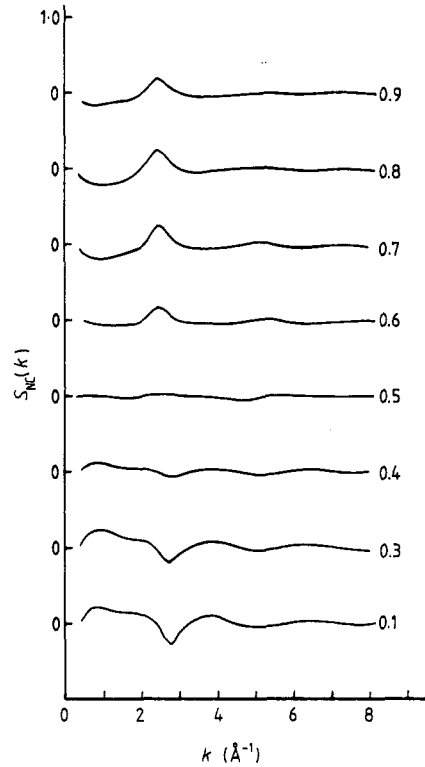


**Figure 5.**  $S_{NC}(k)$  against  $k$  for different atomic fractions of Mg for the Mg-Zn melt.

figure 6, with the help of the Kirkwood-Buff equation. Table 3 presents these results along with the experimental compressibility values of the pure elements [15, 16].

The coefficient of friction, which is essentially the sum of that due to hard-core interaction, soft interaction and cross effect of hard and soft forces, is presented in table

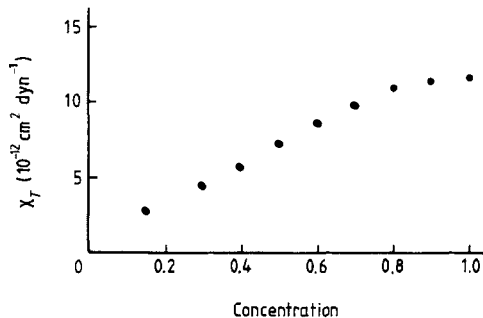


**Figure 6.** Isothermal compressibility ( $\chi_T$ ) against concentration of Mg in the Mg-Zn melt.

**Table 2.** The principal peak height and position of the  $S_{\text{TOTAL}}(k)$  curve.

Temperature	Concentrations or atomic fractions of Mg	Calculated		Experimental	
		Position ( $\text{\AA}^{-1}$ )	Height $S(k)$	Position ( $\text{\AA}^{-1}$ )	Height $S(k)$
926.0	0.15	2.80	2.40	2.80	2.50
	0.30	2.75	2.00	2.75	2.10
	0.40	2.70	2.00	2.70	2.10
	0.50	2.60	1.90	2.60	2.10
	0.60	2.55	1.90	2.60	2.10
	0.70	2.50	1.90	2.60	2.25
	0.80	2.40	2.00	2.45	2.25
	0.90	2.40	2.10	2.40	2.30

**Table 3.** Isothermal compressibility  $\chi_T$ , of Mg–Zn alloy at different atomic fractions of Mg.

Atomic fractions of Mg	$\rho_{11}$ ( $\text{\AA}^3$ )	$\rho_{22}$ ( $\text{\AA}^3$ )	$\rho k_B T \chi_T$	$\chi_T$ ( $10^{-12} \text{ cm}^2 \text{ dyn}^{-1}$ )
0.0001	0.0000	0.0619	0.0133	1.68 (Expt: 2.40)
0.1500	0.0085	0.0484	0.0207	2.83
0.3000	0.0158	0.0369	0.0298	4.43
0.4000	0.0201	0.0302	0.0369	5.74
0.5000	0.0240	0.0240	0.0441	7.17
0.6000	0.0276	0.0184	0.0508	8.64
0.7000	0.0307	0.0132	0.0561	9.96
0.8000	0.0339	0.0085	0.0595	11.10
0.9000	0.0367	0.0047	0.0606	11.40
0.9999	0.0393	0.0000	0.0597	11.80 (Expt: 4.00)

4. The contribution from the hard-sphere part is dominant. The sum of the soft and soft-hard part also contributes significantly.

The self-diffusion coefficients of Mg and Zn are also tabulated in table 4. It is observed that both  $D_{\text{Mg}}$  and  $D_{\text{Zn}}$  increase with increasing Mg concentration. The results

**Table 4.** Calculated diffusion coefficients of Mg–Zn alloy at 926 K.

Concentration (atomic fraction of Mg)	Friction coefficients†						Self-diffusion coefficient‡	
	$\mathcal{E}_i^H/k_B T$		$\mathcal{E}_i^S/k_B T$		$\mathcal{E}_i^{SH}/k_B T$		$D_{\text{Mg}}$	$D_{\text{Zn}}$
	Mg	Zn	Mg	Zn	Mg	Zn		
0.15	0.150	0.202	0.015	0.016	0.026	0.026	5.242	4.098
0.30	0.116	0.155	0.020	0.021	0.030	0.032	5.992	4.789
0.40	0.100	0.132	0.021	0.025	0.039	0.036	5.374	5.182
0.50	0.087	0.114	0.026	0.030	0.042	0.042	5.540	5.370
0.60	0.076	0.099	0.027	0.033	0.042	0.044	6.830	5.653
0.70	0.068	0.087	0.032	0.038	0.044	0.048	6.977	5.785
0.80	0.060	0.077	0.033	0.038	0.044	0.050	7.268	6.034

† In  $10^5 \text{ s cm}^{-2}$ .

‡ In  $10^{-5} \text{ cm}^2 \text{ s}^{-1}$ .



obtained could not be compared due to unavailability of experimental results. The ratio  $D_{\text{Mg}}/D_{\text{Zn}}$  at different atomic fractions of Mg is almost a constant irrespective of the composition of the alloy in conformity with the predictions of regular solution theory [17–19].

At this juncture it may be pointed out that structure factors can also be evaluated through the use of the conventional pseudopotential theory, as suggested by Young [20]. According to him, the pseudopotential perturbation theory, which is valid for unmixed constituents, sometimes has some limitations in its capability to deal with mixed constituents of two metals, i.e. an alloy. However the present approach is a different one. It is a classical approach utilising the random phase approximation (RPA) [21], with a Lebowitz hard-sphere mixture reference system. The present calculations do yield satisfactory results.

It is very important to point out that here the structure factors of the alloy are faithfully reproduced solely from the potential parameters of the pure elements. Hence this method forms a major approach to the investigation of structural properties of liquid alloys. Here the alloy is treated as a mixture formed from 'ideal mixing' of the two constituents. Such a mixture does not involve any charge transfer as in Au–Cs, which is an ionic alloy with salt-like partial structure factors [22].

### Acknowledgments

UB is grateful to the University Grants Commission for a SRF and RVGR to the Department of Science and Technology for financial assistance.

### References

- [1] Lebowitz J C 1964 *Phys. Rev. A* **133** 895
- [2] Baxter R J 1970 *J. Chem. Phys.* **52** 4559
- [3] Gopala Rao R V and Satpathy B M 1982 *Phys. Status Solidi b* **110** 273
- [4] Gopala Rao R V and Das Gupta B 1985 *Phys. Rev. B* **32** 6429
- [5] Ashcroft N W and Langreth D C 1967 *Phys. Rev.* **159** 500
- [6] Kim M G and Letcher S V 1971 *J. Chem. Phys.* **55** 1164
- [7] *Handbook of Chemistry and Physics* 1986–7 63rd edn, ed. R C Weast (Boca Raton, FL: Chemical Rubber) pp B245, 246
- [8] Huijben M J and Vanderlugt W 1979 *Acta Crystallogr. A* **35** 431
- [9] Kirkwood J G and Buff P 1951 *J. Chem. Phys.* **19** 774
- [10] Bhatia A B and Thornton D E 1970 *Phys. Rev. B* **2** 3004
- [11] Helfand E 1961 *Phys. Fluids* **4** 68
- [12] Davis H T and Polyvos P F 1966 *J. Chem. Phys.* **46** 4043
- [13] Waseda Y 1977 *Liquid Metals 1976* (Inst. Phys. Conf. Ser. 30)
- [14] Buhler E, Lampeter P and Steeb S 1987 *Z. Naturf.* **a42** 507
- [15] *Handbook of Chemistry and Physics* 1969–70 50th edn (Cleveland, OH: Chemical Rubber)
- [16] Faber T E 1972 *Introduction to the Theory of Liquid Metals* (Cambridge: CUP)
- [17] Bearman R J and Jones P F 1960 *J. Chem. Phys.* **33** 1432
- [18] Bearman R J 1961 *J. Chem. Phys.* **65** 1961
- [19] Jacucci G and McDonald I R 1975 *Physica A* **80** 607
- [20] Young W H 1987 *Can. J. Phys.* **65** 241
- [21] Pines D and Nozières P 1966 *The Theory of Quantum Liquids* (New York: Benjamin)
- [22] Gopala Rao R V and Bhattacharya M 1987 *Phys. Status Solidi a* **103** 79